Improved Collision Perception Neuronal System Model With Adaptive Inhibition Mechanism and Evolutionary Learning

QINBING FU [1,2,3], (Member, IEEE), **HUATIAN WANG** [2,3], (Student Member, IEEE), **JIGEN PENG** [1,4], AND **SHIGANG YUE** [1,2,3], (Senior Member, IEEE)

[1] Machine Life and Intelligence Research Centre, Guangzhou University, Guangzhou 510006, China
[2] Computational Intelligence Laboratory, School of Computer Science, University of Lincoln, Lincoln LN6 7TS, U.K.
[3] Lincoln Centre for Autonomous Systems, University of Lincoln, Lincoln LN6 7TS, U.K.
[4] School of Mathematics and Information Science, Guangzhou University, Guangzhou 510006, China

Corresponding authors: Qinbing Fu (qifu@lincoln.ac.uk) and Shigang Yue (syue@lincoln.ac.uk)

ABSTRACT Accurate and timely perception of collision in highly variable environments is still a challenging problem for artificial visual systems. As a source of inspiration, the lobula giant movement detectors (LGMDs) in locust's visual pathways have been studied intensively, and modelled as quick collision detectors against challenges from various scenarios including vehicles and robots. However, the state-of-the-art LGMD models have not achieved acceptable robustness to deal with more challenging scenarios like the various vehicle driving scenes, due to the lack of adaptive signal processing mechanisms. To address this problem, we propose an improved neuronal system model, called LGMD$^+$, that is featured by novel modelling of spatiotemporal inhibition dynamics with biological plausibilities including 1) lateral inhibitions with global biases defined by a variant of Gaussian distribution, spatially, and 2) an adaptive feed-forward inhibition mediation pathway, temporally. Accordingly, the LGMD$^+$ performs more effectively to detect merely approaching objects threatening head-on collision risks by appropriately suppressing motion distractors caused by vibrations, near-miss or approaching stimuli with deviations from the centre view. Through evolutionary learning with a systematic dataset of various crash and non-collision driving scenarios, the LGMD$^+$ shows improved robustness outperforming the previous related methods. After evolution, its computational simplicity, flexibility and robustness have also been well demonstrated by real-time experiments of autonomous micro-mobile robots.

INDEX TERMS Lobula giant movement detector, neuronal system model, collision perception, adaptive inhibition, evolutionary learning, highly variable environment.

I. INTRODUCTION

The process of detecting movement is ubiquitous amongst most animals. Millions of years of evolutionary development has endowed, in nature, animals with robust and efficient vision systems capable of collision perception to deal with a variety of aspects of life including foraging, escaping from predators and so forth. Taken a prominent example, locusts can migrate for a long distance in dense swarms containing hundreds to thousands of individuals, free of collision [1].

Despite swarm size, collision rates between locusts are generally low.

In the locust's visual pathways, a group of wide-field movement sensitive neurons, i.e., the lobula giant movement detectors (LGMDs), has been identified to respond most strongly to divergence of image edges by approaching objects on a direct collision course rather than any other categories of movements [2]–[6]. More precisely, the LGMD releases bursts of energy whenever a locust is on a collision course with its cohorts or a predator bird. These energy by neural pulses prompt the locusts to take evasive actions. The entire process from collision perception to reaction takes less than 50 milliseconds [7], [8]. Therefore, as an excellent paradigm,

The associate editor coordinating the review of this manuscript and approving it for publication was Haiquan Zhao [ID].

Q. Fu *et al.*: Improved Collision Perception Neuronal System Model With Adaptive Inhibition Mechanism and Evolutionary Learning

IEEE *Access*

the LGMD has been studied intensively, and built as quick collision detectors with a good number of models and applications [9], [10].

Although the LGMD's efficacy has been validated with challenges from different scenarios including the ground vehicles [11]–[17], robots [18]–[25], and unmanned aerial vehicles (UAV) [26], [27], the models have been tested mostly with indoor (lab) scenes, rarely with on-road or outdoor situations. The robustness to deal with highly variable statistics of complex environments has not achieved an acceptable level, due to the lack of adaptive signal processing mechanisms. As a result, the current models are noise sensitive to visual stimuli caused by vibrations, cluttered optic flows in periphery field of view, near-miss or approaching objects with deviations from the centre view. The models usually respond strongly to a non-collision event or miss a sudden collision risk from a complex dynamic background, both of which are not expected for an accurate collision perception visual system. To improve the robustness of LGMD models functioning in more challenging visual environments full of irrelevant background optic flows or motion distractors, the LGMD's computational structure should be more adaptable and robust.
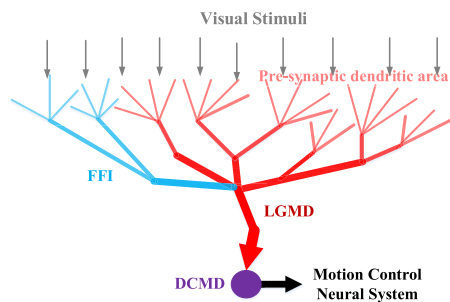

FIGURE 1. Schematic illustration of the LGMD's neuromorphology: the pre-synaptic dendritic area consists of two main fields of motion dependent excitation (red) and feed-forward inhibition (blue). The DCMD is a one-to-one post-synaptic neuron relaying the LGMD's energy to motor. A locust has this neural structure in either side of bilateral eyes.

From both the biologists' and modellers' perspectives [5], [9], the spatiotemporal competitive interactions between two kinds of signal flows, i.e., the excitation and the inhibition, play crucial roles of shaping the LGMD's specific collision selectivity. More concretely, the excitation is motion dependent (see Fig. 1), and generates the lateral inhibitions which spread out to surrounding areas with respect to time, and then cuts down the excitations at the same place. In addition, there is another individual inhibition pathway reliant on moving object size, called the feed-forward inhibition (FFI, see Fig. 1). In previous LGMD models and neural networks, the lateral inhibition possesses the constant bias, in space, interacting with the excitation; and the FFI obeys an 'all-or-none' law with hard thresholding that can directly shut down the firing of LGMD at some critical moments like the end of approaching or the start of receding. When dealing with visual environments like the indoor or laboratory scenes, those inhibition mechanisms are effective to mediate the

LGMD's responsive preference to moving objects signalling collision. However, we have noticed that those can not fulfil the accurate and timely perception of collision in more challenging backgrounds like the various vehicle driving scenes of varying lighting or weather conditions.

To address this problem, we propose a new LGMD model, called **LGMD$^+$**. Compared to all the related methods, our emphasis is laid on the implementation of spatiotemporal inhibition dynamics to fit with the perception of collision in highly variable environments, which includes the following new bio-plausible mechanisms:

1) With a hypothesis of position dependent mechanism compensating for the differences in visual input density [28], the lateral inhibitions have spatially varying bias within the whole field of view that is defined by a variant of Gaussian distribution resulting in higher sensitivity around the centre view over the peripheries. This works effectively to suppress peripheral irrelevant optic flows, to a great extent.

2) An adaptive inhibition mechanism via the FFI pathway tunes both the strength of lateral inhibitions and the latency of local excitations before reaching the LGMD cell, temporally, rather than directly shutting down the LGMD. This makes the model more adaptable to deal with highly variable statistics of environments for extracting the process of approach.

Moreover, we also apply evolutionary learning algorithms to tune the proposed LGMD$^+$ using our collected dataset of on-road driving scenarios consisting of hundreds of first-view video clips adapted or recorded from dashboard cameras.[1] Evolving with two representative LGMD models [14], [29] for competition, the LGMD$^+$ demonstrates improved robustness. After the evolutionary tuning, the effectiveness of LGMD$^+$ is validated with a good number of new off-line driving scenes. It is also implemented in the embedded vision of micro-mobile robots. The on-line multi-robot experiments also verify its computational simplicity and flexibility.

The remainder of the paper is structured as follows: A survey on the most related neural-based collision perception approaches is summarised in Section II. Section III elucidates the proposed neuronal system model and learning methods. Section IV introduces the experimental settings. Section V reports on the artificial evolutions and the verification experiments after the evolution. Section VI discusses the characterisation of proposed LGMD$^+$ and existing challenges. Section VII concludes this research.

II. RELATED WORK

Within this section, we review briefly the most related works in the areas of 1) collision perception visual methods inspired by flying insects, and 2) typical LGMD neuronal system models for collision perception and avoidance.

---

[1]The dataset and the representations of model layers & channels are accessible in https://github.com/fuqinbing/LGMD-Plus-and-GAs-Open-Source.

IEEE *Access*

Q. Fu *et al.*: Improved Collision Perception Neuronal System Model With Adaptive Inhibition Mechanism and Evolutionary Learning

(a) The comparative LGMD-S model in [29]   (b) The comparative LGMD-D model in [14]   (c) The proposed LGMD$^+$ model
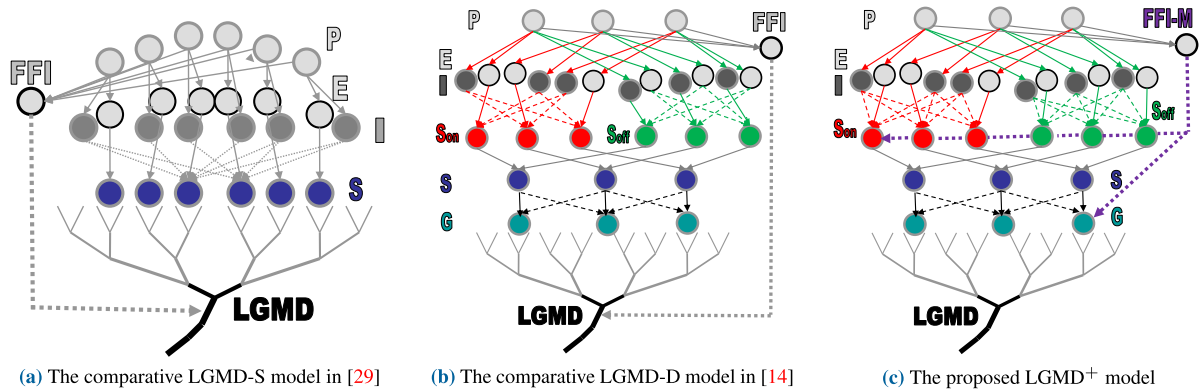
FIGURE 2. Schematic illustrations of the two comparative LGMD models and the proposed LGMD$^+$ model in order to highlight the key differences in structure. The dashed lines indicate delayed processes. Only several cells are taken from the visual field to exemplify each processing.

TABLE 1. Nomenclature in this paper.

acronym	full name
LGMD	lobula giant movement detector
DCMD	descending contra-lateral motion detector
FFI(-M)	feed-forward inhibition(-mediation)
LGMD-S	LGMD single-pathway
LGMD-D	LGMD dual-pathways
GA	genetic algorithm

A. BIO-INSPIRED VISION FOR COLLISION PERCEPTION

Inspired by flying insects, there have been a few categories of visual systems specialising in collision perception [9], [10]. Firstly, a good number of approaches come from the well-known optic flow-based theories in fruit flies and bees, e.g., [30]–[32], which mimics the functions of bilateral compound eyes of flying insects at ommatidia (optical units) level. These approaches are suitable for detecting lateral collision threats, and have been widely used in near range navigation of flying robots and micro-air vehicles [33], and reviewed in [34], [35].

Another type of models and neural networks originates from the locust's visual pathways [5], [9]. The LGMD-1 (namely LGMD in this paper) was firstly investigated as many quick collision-detecting visual systems with different theories shaping its specific collision selectivity (e.g., [3], [14], [20], [21], [36]). Some methods have been successfully applied in ground robots [25], [37]–[41], and UAV [26], [27]. Recently, an LGMD's neighbouring partner – the LGMD-2, with unique responsive preference to only darker approaching objects relative to the background, has also been built as quick collision selective neuronal system models with implementation in micro-robots [23], [24], [42], [43].

Moreover, the directionally selective neurons found in the locust's visual pathways [44], with specific sensitivity to directional movements, have been modelled as collision perception visual neural networks by integrating different directionally selective neurons that can tell the primary direction of proximity [29], [45].

B. LGMD MODELS

Collision perception and subsequent avoidance are two separate vital phases for the survival of both animals and mobile machines. Based on LGMD, the vast majority of methods including the proposed LGMD$^+$ concentrate on the stage of perception. Accordingly, we herein present a few state-of-the-art LGMD models with emphasis placed on the neural basis of perception and avoidance, respectively.

Firstly, the two LGMD models, illustrated in Fig. 2, represent two theoretical frameworks, as the comparative models in this research. The LGMD-S model processes visual information in a single pathway with four layers, the photoreceptor (P), the excitation (E), the inhibition (I), and the summation (S) layers, and two cells, the FFI and the LGMD (see Fig. 2a) [29]. It is a fundamental structure that depicts the competitive interaction between the excitation and delayed inhibition to form the LGMD's specific selectivity. This model with its different extensions have been widely applied in ground robots and UAV, as reviewed in [9]. Differently to the LGMD-S, the LGMD-D model is a seminal work that demonstrates the functionality of ON and OFF dual-pathways to implement a locust's LGMD [14]. This model splits motion signals into parallel neural computation: the brightness increments flow into the ON pathway, whilst the decrements stream into the OFF pathway. Moreover, the parallel processing of ON and OFF contrast also for the first time realises the functionality of its neighbouring LGMD-2, with validation in vehicle and robot scenarios [23].

On the aspect of avoidance, the underlying circuits and mechanisms in locusts remain largely unknown. Although many of the LGMD models have been satisfactorily applied for conducting the robot's collision avoidance, the control strategies are generally simple. For wheeled robots, a directional escape method was proposed in two works [38], [43], by the division of the visual field handled by two separate LGMDs. More precisely, the first firing of left or right-side LGMD guides the reactive avoidance to the right or left, after the perception. Recently, a more complex learning based control strategy was successfully combined with the LGMD in
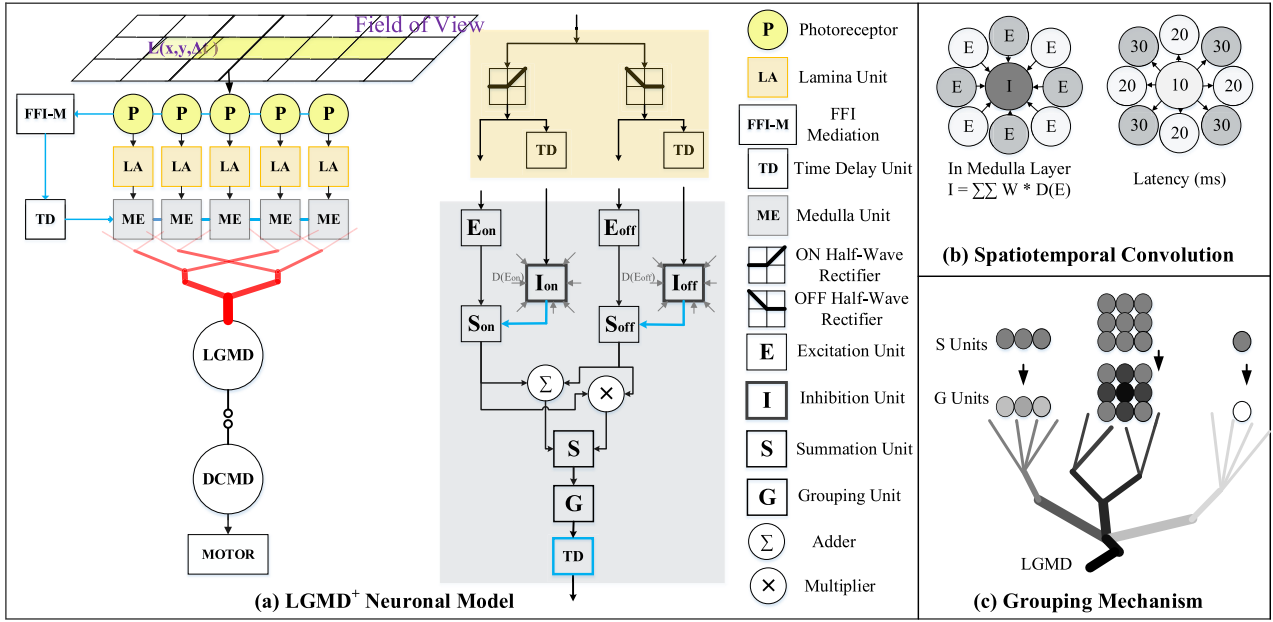
Q. Fu *et al.*: Improved Collision Perception Neuronal System Model With Adaptive Inhibition Mechanism and Evolutionary Learning

IEEE *Access*

FIGURE 3. Schematics of (a) the neuronal system LGMD$^+$ model, with (b) the spatiotemporal convolution, and (c) the grouping mechanism. Only five cells are taken from the field of view to exemplify the visual processing. The blue pathway originating in the Retina layer indicates the tuning of FFI-M in the Medulla layer.

a hexapod walking robot, with validation in interception avoidance scenarios [25], [41]. Importantly, this work presents an end-to-end structure of bio-inspired neural networks connecting both the perception and avoidance steps.

III. METHODS

In this section, we elucidate 1) the formulation of LGMD$^+$, and 2) the evolutionary learning algorithms.

A. FORMULATION OF THE MODEL

Differently to all the previous methods, and building upon a preliminary modelling work in [46], the emphasis of LGMD$^+$ herein is laid on the modelling of spatiotemporal inhibition dynamics to more effectively affect the excitation in order to improve the robustness in highly variable environments. In general, the LGMD$^+$ processes visual signals in a feed-forward manner mimicking the locust's looming sensitive visual pathways, through several neuropile layers including **Retina**, **Lamina**, **Medulla**, and **Lobula**. Fig. 3 illustrates the schematic of LGMD$^+$ neuronal system model.

1) COMPUTATIONAL RETINA LAYER

As illustrated in Fig. 3, the first Retina layer of insect's visual systems is composed of photoreceptors, arranged in a matrix sensing time-varying luminance (green-channel or grey-scale in our case). Let $L(x, y, t) \in \mathbb{R}^3$ denote the input image streams, where x, y and t are spatial and temporal positions. This layer computes temporal derivative of every pixel to get

the motion information, as the following:

$$P(x, y, t) = L(x, y, t) - L(x, y, t-1) + \sum_{i=1}^{n_p} a_i P(x, y, t-i), \quad (1)$$

$$a_i = \left(1 + e^i\right)^{-1}. \quad (2)$$

The persistence of luminance change could last for a short while of n_p number of frames, and a_i is the decay coefficient.

Following that, the motion is blurred through a spatial Gaussian filter. The calculation is given by

$$\hat{P}(x, y, t) = \sum_{u=-1}^{1} \sum_{v=-1}^{1} P(x - u, y - v, t) \cdot G_{\sigma_1}(u, v), \quad (3)$$

$$G_{\sigma_1}(u, v) = \frac{1}{2\pi \sigma_1^2} \exp\left(-\frac{u^2 + v^2}{2\sigma_1^2}\right). \quad (4)$$

2) COMPUTATIONAL LAMINA LAYER

Motion information induces luminance increment or decrement over time. As shown in Fig. 3, there are lamina units or rectifying transient cells separating the relayed signals into parallel channels. More precisely, the luminance increment flows into the ON channel, whilst the decrement streams to the OFF channel. That is,

$$\hat{P}_{on}(x, y, t) = [\hat{P}(x, y, t)]^+ + \alpha_1 \hat{P}_{on}(x, y, t - 1),$$
$$\hat{P}_{off}(x, y, t) = -[\hat{P}(x, y, t)]^- + \alpha_1 \hat{P}_{off}(x, y, t - 1). \quad (5)$$

$[x]^+$ and $[x]^-$ denote $\max(0, x)$ and $\min(x, 0)$. A small fraction (α_1) of motion, at the previous time as the residual information, is allowed to pass through.

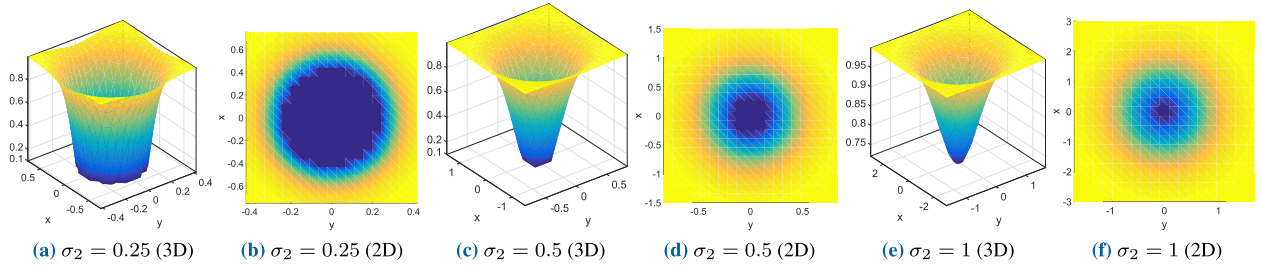| (a) $\sigma_2 = 0.25$ (3D) | (b) $\sigma_2 = 0.25$ (2D) | (c) $\sigma_2 = 0.5$ (3D) | (d) $\sigma_2 = 0.5$ (2D) | (e) $\sigma_2 = 1$ (3D) | (f) $\sigma_2 = 1$ (2D) |

FIGURE 4. [B] bias distribution on the whole visual field with three individual standard deviations: the dark-to-light region represents the bias of low-to-high grade.

3) COMPUTATIONAL MEDULLA LAYER

The Medulla layer is the place where the LGMD's specific collision selectivity is formed by the competition between excitations and inhibitions in both the ON and OFF channels. Firstly, in the ON channels, the local excitation reaches the E_{on} unit without temporal latency; meanwhile, it is fed into a time delay unit (TD in Fig. 3), represented by a first-order low-pass filtering. The lateral inhibition is formed by convolving surrounding delayed excitations $\hat{E}_{on}$ (see $D(E)$ in Fig. 3). The whole process can be defined as the following:

$$E_{on}(x, y, t) = \hat{P}_{on}(x, y, t), \tag{6}$$

$$\hat{E}_{on}(x, y, t) = \alpha_2 E_{on}(x, y, t) + (1 - \alpha_2) E_{on}(x, y, t-1), \tag{7}$$

$$\alpha_2 = \tau_i / (\tau_e + \tau_i), \tag{8}$$

$$I_{on}(x, y, t) = \sum_{i=-1}^{1} \sum_{j=-1}^{1} \hat{E}_{on}(x+i, y+j, t) \cdot W_i(i, j). \tag{9}$$

τ_e and τ_i are two time constants in milliseconds, wherein τ_e stands for the excitation delay time (see Fig. 3(b)) and τ_i is the time interval between successive frames of digital signals. W_i denotes a convolution kernel, defined by

$$W_i = \begin{bmatrix} 1/8 & 1/4 & 1/8 \\ 1/4 & 1 & 1/4 \\ 1/8 & 1/4 & 1/8 \end{bmatrix}. \tag{10}$$

Notably, in the convolution process, the centre cell has the greatest weighting and shortest delay; the four nearest cells have the moderate weighting and delay; the four diagonal cells share the lowest weighting and longest delay (see Fig. 3(b)). The selection of spatiotemporal parameters takes reference from a biological research [5]: the excitation is delayed, when spreading out to its surrounding area to form the lateral inhibitions, and cutting down the excitations at the same place. The generation of local excitations and lateral inhibitions in the OFF channels conforms to the neural computations of ON channels, which is omitted here. After that, there are local summation units in both polarity pathways. The computations are defined as

$$S_{on}(x, y, t) = [E_{on}(x, y, t) - w_1(t) \cdot I_{on}(x, y, t) \cdot B(x, y)]^+,$$
$$S_{off}(x, y, t) = [E_{off}(x, y, t) - w_1(t) \cdot I_{off}(x, y, t) \cdot B(x, y)]^+ \tag{11}$$

It is worth emphasising that **the proposed spatiotemporal inhibition dynamics is mainly reflected here**: $w_1(t)$ is a time-varying local bias to adjust the strength of lateral inhibition; [B] is a global spatial bias matrix, in which the position dependent bias is defined by a variant of Gaussian distribution on the view. In addition, only the non-negative excitations are retained.

More specifically, the lateral inhibitions are tuned by an FFI-mediation (FFI-M) pathway originating in the Retina layer (see Fig. 3(a)). The functions are defined as

$$F(t) = \sum_{x=1}^{R} \sum_{y=1}^{C} |P(x, y, t)| \cdot (C \cdot R)^{-1}, \tag{12}$$

$$\hat{F}(t) = \alpha_3 F(t) + (1 - \alpha_3) F(t-1), \quad \alpha_3 = \tau_i / (\tau_f + \tau_i), \tag{13}$$

$$w_1(t) = \max\left(w_2, \frac{\hat{F}(t)}{T_f}\right). \tag{14}$$

C and R indicate the columns and rows of the visual field; w_2 denotes a baseline for the local bias; τ_f indicates a latency in milliseconds; T_f stands for a threshold. Consequently, the lateral inhibitions will get more powerful, if luminance changes intensely over the field of vision.

Secondly, the spatially varying bias matrix [B] affects lateral inhibitions, at local pixel level. That is,

$$B(x, y) = \max\left(w_3, 1 - G_{\sigma_2}(x, y)\right), \tag{15}$$

$$G_{\sigma_2}(x, y) = \frac{1}{2\pi \sigma_2^2} \exp\left(-\frac{x^2 + y^2}{2\sigma_2^2}\right). \tag{16}$$

w_3 denotes a baseline in the bias matrix. Fig. 4 exemplifies three individual [B] distributions, in which σ_2 adjusts the sensitivity over the view. More precisely, the larger standard deviation gives rise to more concentrated area around the centre view influenced by lower biases; whilst the surrounding region is with relatively higher biases.

Subsequently, there is a supralinear interaction between the ON and OFF local excitations, at every summation unit (see Fig. 3). That is,

$$S(x, y, t) = \theta_1 S_{on}(x, y, t) + \theta_2 S_{off}(x, y, t)$$
$$+ \theta_3 S_{on}(x, y, t) S_{off}(x, y, t), \tag{17}$$

Q. Fu *et al.*: Improved Collision Perception Neuronal System Model With Adaptive Inhibition Mechanism and Evolutionary Learning

IEEE *Access*

where $\{\theta_1, \theta_2, \theta_3\}$ denotes the combination of term coefficients which can implement both linear and multiplicative operations.

Cascaded the S unit, a grouping unit is introduced to reduce isolated noise in cluttered backgrounds (see Fig. 3(c)). This is implemented with a passing coefficient matrix $[Ce]$, determined by a convolution with an equally weighted kernel, as the following:

$$Ce(x, y, t) = \sum_{i=-1}^{1} \sum_{j=-1}^{1} S(x+i, y+j, t) \cdot W_g(i, j), \quad (18)$$

$$W_g = \frac{1}{9} \times \begin{bmatrix} 1 & 1 & 1 \\ 1 & 1 & 1 \\ 1 & 1 & 1 \end{bmatrix}, \quad (19)$$

$$G(x, y, t) = S(x, y, t) \cdot Ce(x, y, t) \cdot \omega(t)^{-1}, \quad (20)$$

$$\omega(t) = \max([Ce]_t) \cdot C_\omega^{-1} + \Delta_C. \quad (21)$$

ω is a scale parameter, updated at every frame; C_ω is a constant coefficient; Δ_C stands for a small real number. Furthermore, the local excitation from the G unit is delayed and sieved by

$$\hat{G}(x, y, t) = \begin{cases} \alpha_4 G(x, y, t) + (1 - \alpha_4)G(x, y, t-1), \\ \quad \text{if } G(x, y, t) \cdot C_{de} \geq T_{de} \\ 0, \quad \text{otherwise} \end{cases} \quad (22)$$

$$\alpha_4 = \tau_i/(\hat{\tau}_g + \tau_i), \quad \hat{\tau}_g = \tau_g \cdot \left[1 - \frac{\hat{F}(t)}{T_f}\right]^+, \quad (23)$$

where C_{de} stands for the decay coefficient, where $C_{de} \in (0, 1)$; T_{de} denotes the decay threshold. Notably, **the FFI-M pathway also tunes the latency of local excitations before arriving the LGMD** (see TD in Fig. 3), where the delay is updated at every frame by a non-negative coefficient. This dynamic temporal tuning indicates that the delay of local excitations will become shorter as the objects growing on the field of view, i.e., the excitation during the process of proximity will be amplified [46]. This is indeed consistent with the biological hypothesis proposed in [5].

4) COMPUTATIONAL LOBULA LAYER

In the Lobula area, an LGMD cell integrates all pre-synaptic local excitations from the G units (see Fig. 3), so as to generate the membrane potential as the following:

$$k(t) = \sum_{x=1}^{R} \sum_{y=1}^{C} \hat{G}(x, y, t), \quad K(t) = \left(1 + e^{-k(t) \cdot (C \cdot R \cdot \alpha_5)^{-1}}\right)^{-1}, \quad (24)$$

where α_5 denotes a scale coefficient, and the output is normalised within $[0.5, 1)$. Subsequently, a spike frequency adaptation mechanism is applied to further sharpen up the LGMD's firing selectivity. That is,

$$\hat{K}(t) = \begin{cases} \alpha_6(\hat{K}(t-1) + K(t) - K(t-1)), \\ \quad \text{if } (K(t) - K(t-1)) \leq T_{sf} \\ \alpha_6 K(t), \quad \text{otherwise} \end{cases} \quad (25)$$

$$\alpha_6 = \tau_s/(\tau_s + \tau_i), \quad (26)$$

where α_6 is a coefficient that indicates the adaptation rate to visual stimuli; T_{sf} denotes a small real number as the threshold; τ_s is a time constant in milliseconds. Generally speaking, the mechanism is a reduction of neuronal response to stimuli with constant or decreasing intensity, e.g., objects recede or translate; while it has little effect on stimuli with increasing intensity like the approach.

The membrane potential is finally exponentially mapped to spikes by an integer-valued function. That is,

$$Spi(t) = \left[e^{(\alpha_7 \cdot (\hat{K}(t) - T_{sp}))}\right], \quad (27)$$

where T_{sp} denotes the spiking threshold, and α_7 is a scale coefficient affecting the firing rate, i.e., raising it will bring about more spikes within a specified time window.

5) DCMD

As illustrated in Fig. 3, the elicited spikes of LGMD is conveyed through a one-to-one synapse connection to the DCMD linking to succeeding motor. We compute the DCMD's spike frequency as the LGMD$^+$ model output in order to indicate the perception of a potential collision threat.

$$Col(t) = \begin{cases} \text{True}, \quad \text{if } \left(\sum_{i=t-n_t}^{t} Spi(i)\right) \times 1000/(n_t \cdot \tau_i) \geq T_c \\ \text{False}, \quad \text{otherwise} \end{cases} \quad (28)$$

n_t denotes the specified time window in frames, and T_c stands for a warning threshold for collision risks.

TABLE 2. Setting parameters of the LGMD$^+$ model.

Parameter	Description	Value
n_p	persistence in Eq. 1	$0 \sim 2$
σ_1	standard deviation in Eq. 3	1
α_1	coefficient in Eq. 5	0.1
τ_i	constant time interval	33.33ms
C, R	columns, rows	adaptable
τ_f	delay constant in Eq. 13	10ms
w_3	baseline bias in Eq. 15	0.1
$\{\theta_1, \theta_2, \theta_3\}$	term coefficients in Eq. 17	$\{1, 1, 0\}$
C_ω	constant in Eq. 21	4
Δ_C	real number in Eq. 21	0.01
C_{de}	decay coefficient in Eq. 22	0.5
τ_g	raw delay in Eq. 23	10ms
T_{sf}	small threshold in Eq. 25	0.003
α_7	scale coefficient in Eq. 27	10
n_t	time window in Eq. 28	10

6) SETTING PARAMETERS

The proposed LGMD$^+$ processes visual signals in a feed-forward structure. The parameters are set up via two ways: partial ones are decided with previous modelling experience that are given in Table 2, and the adaptable ones are searched

IEEE Access

Q. Fu *et al.*: Improved Collision Perception Neuronal System Model With Adaptive Inhibition Mechanism and Evolutionary Learning

by evolutionary learning, including the temporal parameters ($\tau_s \in [300, 1300]$ms in Eq. 26, $\tau_e \in [1, 50]$ms in Eq. 8), the core mechanism coefficients ($w_2 \in [0.1, 2.0]$ in Eq. 14, $\alpha_5 \in [0.1, 2.0]$ in Eq. 24, $\sigma_2 \in [0.1, 2.0]$ in Eq. 15), and the thresholds ($T_c \in [20, 150]$ in Eq. 28, $T_f \in [5, 30]$ in Eq. 14, $T_{sp} \in [0.6, 0.95]$ in Eq. 27, $T_{de} \in [5, 50]$ in Eq. 22). The C, R are set differently in off-line and on-line experiments. The distributions of a few adaptable parameters during evolutions are depicted in Fig. 7 and 9.

B. ARTIFICIAL EVOLUTION

To make the LGMD$^+$ more adaptable to various variable environments, we apply the evolutionary learning to simulate the natural evolving of biological visual systems. To be more specific, we utilise the genetic algorithm (GA), as optimisation method to tune the adaptable parameters. The GA is based on natural phenomenon that applies nature inspired approaches including survival of the fittest, and operators such as the selection, paring, crossover and mutation [47].

Specifically for this research, the GA is implemented on the basis of following observations:

1) We can define a good population of model agents each with a random set of parameters, as the search space to investigate the performance in various highly variable environments.
2) The GA is able to provide a list of 'good' solutions rather than a single one after development.
3) We can compare the competence of different models evolving together in a same setting of visual environments.

To demonstrate the improved robustness of the proposed LGMD$^+$, we compare two typical LGMD models, as shown in Fig. 2. In addition, we choose two evolutionary learning strategies:

1) Individual evolution: agents from each type of models evolve, individually and over many generations.
2) Competitive coevolution: all participant model agents are developing together; each group exerts selective pressures on the others, thereby affecting each other's evolution [48], [49]. Consequently, the two comparative models and the proposed model compete for a superior role of timely and accurate perception of collision risks, all aiming at retaining more agents survival in the whole population.

1) GA PHASES

The whole process is introduced in Algorithm 1. To elaborate on that, a population of $p = 20$ or $p = 40$ agents in each generation is processed through entire $m = 100$ or $m = 50$ generations. The first generation is produced randomly, in which each agent possesses a chain of parameters laying within the corresponding ranges. Every set of parameters is called a 'chromosome' by genetics terminology, and every single parameter represents a 'gene'. To form a new generation, the worst-performing agents ($20\% \times p$)

Algorithm 1 GA Phases

Input: Initial a population (p) of agents each with a random set of genes and generation $g = 1$

Output: Survived agents each with a set of optimised genes and fitness *Fit* over $g = m$ generations

1 Run input visual dataset (for all agents);
2 Calculate each agent's *Fit* (in descending order);
3 **while** $g \leq m$ **do**
4   Select n agents as parents with top ranking *Fit*;
5   Pairing and crossover with local probability P_c to bear $n/2$ offsprings;
6   Mutation on offsprings with local probability P_m;
7   Run input visual dataset (for descendents);
8   Calculate new *Fit* and rank all (in descending order);
9   Select $p - n/2$ survivors with higher ranking *Fit*, then eliminate others;
10   Update generation $g + 1$;
11 **end**
12 Return the evolved agents;

---

are substituted. The descendents ($20\% \times p$) are produced by the best-performing agents, selected as parents from the previous generation through the crossover. An uniform-crossover strategy herein is applied with a large local probability set to $P_c \in [0.8, 0.9]$ on each gene [50]. The mutation that represents small stochastic tweak in the chromosome is made to each gene with a small local probability set to $P_m \in [0.2, 0.3]$. It is implemented by a Gaussian perturbation theory, since each gene is encoded by floating number rather than binary code. Precisely speaking, let the raw gene x be the mean, the mutated gene $\hat{x}$ with deviation from the mean x can be obtained by

$$\hat{x} = x \pm \frac{\sqrt{d} \cdot x}{3\sigma_3}, \quad d = -2 \cdot \sigma_3^2 \cdot \ln\left(\sqrt{2\pi\sigma_3^2} \cdot \eta\right), \quad (29)$$

$$\eta \in \left[\frac{1}{\sqrt{2\pi\sigma_3^2}}\exp\left(-\frac{(3\sigma_3)^2}{2\sigma_3^2}\right), \frac{1}{\sqrt{2\pi\sigma_3^2}}\right], \quad (30)$$

where the standard deviation σ_3 is set at 1, and η denotes a random likelihood. In the GA, the mutation operation plays an important role to enlarge the searching pool and avoid prematurity, i.e., the algorithm converges too early. In addition to that, though the worst-performing agents are driven to extinction, the mutation may bring the extinct agents back again in subsequent generations.

The process of competitive coevolution are similar to the Algorithm 1, except that the best-performing parents to bear offsprings are selected from the population with top ranking average fitness, and the worst-performing agents from the population with bottom ranking average fitness are eliminated from the competition. Consequently, the

Q. Fu *et al.*: Improved Collision Perception Neuronal System Model With Adaptive Inhibition Mechanism and Evolutionary Learning

IEEE *Access*

best-performing model population could dominate the whole population, and leave little chance for others to survive.

2) FITNESS FUNCTION

The term of 'fitness' is worth to be stressed, since it is the function we aim to optimise and use to evaluate each agent's behaviour for selecting the most promising solutions. Therefore, a good design of fitness function determines a satisfactory evolutionary learning. In this research, the correct perception rate (CPR) or success rate (SR) is the only criterion – whether the agent can discriminate properly between collision and non-collision incidents, corresponding to the accurate and timely perception of collision risks. The fitness of an i-th agent in the population is given by

$$Fit(i) = \left(1 - \frac{F_{col}(i) \cdot S_{col} + F_{non}(i) \cdot S_{non}}{N_{col} \cdot S_{col} + N_{non} \cdot S_{non}}\right) \times 100\%, \quad (31)$$

where $F_{col}(i)$ and $F_{non}(i)$ stand for the failures of collision perception and the false alert for non-collision events; N_{col} and N_{non} denote the total amount of collision and non-collision events; $S_{col} = 3$ and $S_{non} = 1$ indicate the corresponding penalty weights. For a collision event, the failure means no warning signal is sent out by the agent, $0 \sim 30$ frames before the labelled ground truth colliding moment, or the signal is later than it; whilst for a non-collision event, the failure indicates the agent signals a collision-like response. Importantly, the failure of collision perception has a higher penalty (threefold the non-collision case), as it is prioritised.

IV. EXPERIMENTAL SETTING

Within this section, we introduce the experimental settings including off-line and on-line tests. Generally speaking, each type of the artificial evolution courses is implemented with four separate rounds. After evolutionary tuning, as the verification experiments, the evolved populations of the two comparative models and the LGMD$^+$ are examined by a good number of new testing scenarios. The evolved LGMD$^+$ agents are also embodied in micro-mobile robots, with validation in on-line multi-robot arena tests.

A. OFF-LINE SETTING

Compared to previous studies, we set up a more comprehensive dataset covering various on-road collision and non-collision scenarios for testing the neuronal system models. Concretely speaking, the visual dataset is divided into two parts, the evolution and the testing environments. Firstly, to cultivate well performing agents capable of adapting to various visual backgrounds, the evolution environment should comprise as many typical events as possible. By leveraging the time costing and the performance, the evolution environment consists of 40 on-road critical moments in total with 30 collision events and 10 non-collision challenges (near-miss, strong background cluttered flows and approach with deviations from the centre view). Secondly, the testing environment consists of 87 new on-road events including 51 crash
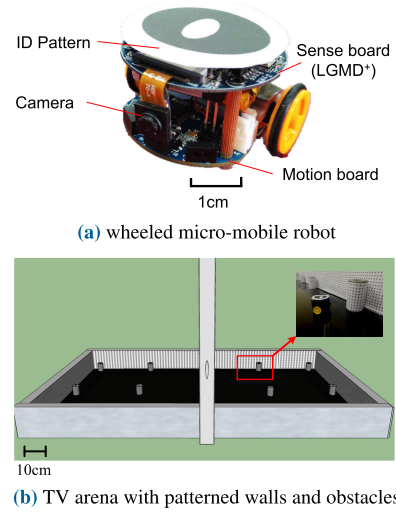

(a) wheeled micro-mobile robot

(b) TV arena with patterned walls and obstacles

FIGURE 5. Illustration of the micro-robot and the arena used in on-line tests. The ID-specific pattern on top of the robot is used for localisation [51].

scenes and 36 non-collision or near-miss cases. All the input visual stimuli are with 432×240 in image resolution, each at 30Hz, and in around 10~30 seconds. The example video clips are shown with results in Section V.

B. ROBOT CONFIGURATION

In this subsection, we introduce the micro-mobile robot and the arena used in the on-line experiments, as illustrated in Fig. 5. The robot is called '*Colias*', which is a vision-based, low-cost, and autonomous wheeled mobile platform (see Fig. 5a). The robot has a small footprint of 4cm in diameter, and 3cm in height. The bottom motion board serves the robot with a maximum speed of roughly 35cm/s, and autonomy of approximately 1 hour. The upper sense board is assembled with a monocular camera (OV7670) system handling the required in-chip image processing, as the only sensor used in this research. The acquired image is set at 99×72 in YUV422 format, at 30Hz. The 32-bit MCU STM32F427, clocked at 180 MHz, provides the necessary computational power to have a real-time image stream processing. Its 256 KB internal SRAM supports the image buffering and computing. Moreover, the visual coverage of camera could reach up to 70 degrees. More detailed configuration of the *Colias* robot can be found in a recent work [39].

Fig. 5b depicts the 3D-profile of arena built on a LCD TV screen. It is with the size of 143 (in length) $\times$ 80.5 (in width) $\times$ 15 (in height) cm^3. A CCD camera is set on the top of arena to record the experiments.

In the on-line experiments, multiple robots function together and interact with each other, as well as the patterned obstacles and peripheral walls for collision perception and avoidance. Six robot agents are applied, each with a distinct set of optimised parameters selected from the last generation of evolved LGMD$^+$ population, after off-line evolutionary tuning. Since the emphasis herein is laid on the perception
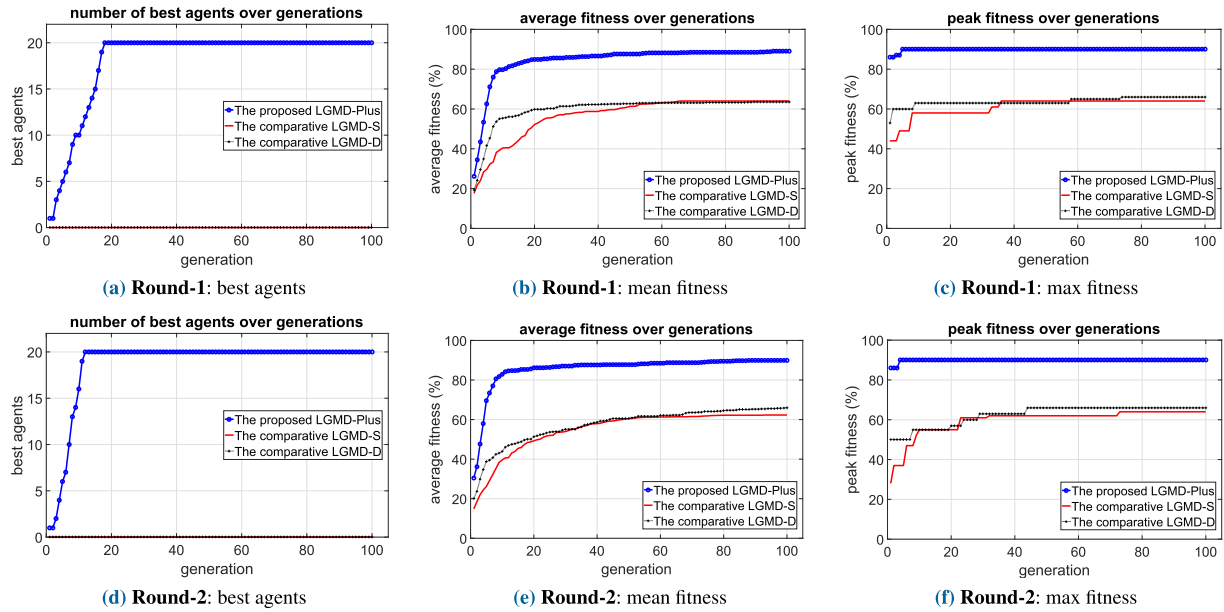
FIGURE 6. Individual evolution results (two rounds) of the proposed LGMD$^+$ and the comparative LGMD populations, each with 20 agents over 100 generations. The number of best agents (with fitness no less than 80%), average and maximum fitness during evolution are shown.
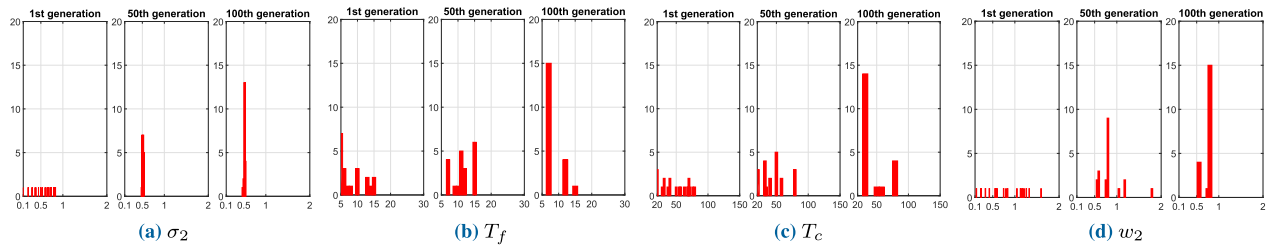

FIGURE 7. Distributions of the four core genes in the investigated LGMD$^+$ population at the 1st, 50th and 100th generations in Fig. 6, including (a) the standard deviation σ_2 in Eq. 16, (b) the threshold T_f in Eq. 14, (c) the threshold T_c in Eq. 28, and (d) the baseline bias w_2 in Eq. 14.

of collision, the motion control including avoidance strategy is simple: each agent is initialised to go forward and wander in the arena, at the linear speed of around 12 cm/s, until a potential collision detected; the avoidance behaviour is set to turn a large angle randomly to the left or right side; after turning, the agent resumes to go forward and so on. Note that only when the agent failed in collision perception resulting in crash with obstacles, walls or other agents, we manually intervened to replace the robot or obstacle.

V. RESULTS

Within this section, we report on the experimental results. Firstly, the two kinds of artificial evolutions with distributions of a few developing parameters, and the best-agent performance on typical training scenes are illustrated. Secondly, the verification of new testing scenes is given. At last, the verification of on-line multi-robot arena test is shown.

A. RESULTS OF ARTIFICIAL EVOLUTIONS
1) INDIVIDUAL EVOLUTION RESULTS
Firstly, for each group of LGMD models evolving individually not affecting each other, the results in Fig. 6 and 8

clearly show that the proposed LGMD$^+$ population out-performs both the comparative models, in all four rounds of evolutions, i.e., the LGMD$^+$ develops consistently with improving robustness to survive in the evolution environment, at different populations. The fitness of LGMD$^+$ population increases constantly, in every round. More precisely, after around 10 generations, the mean fitness of the LGMD$^+$ population surpasses a high degree, **80%**, that is used to define the standard of becoming a 'best agent'; on the other hand, the mean fitness of the two comparative model populations can only reach above 60%, after approximate 40 generations. In every generation, the maximum fitness of the LGMD$^+$ population is much greater than the other two populations. Most importantly, after $10 \sim 30$ generations, the LGMD$^+$ evolving agents have been all promoted to the 'best agents'; whilst there are no 'best agents' for the two comparative LGMD populations.

Moreover, Fig. 7 and 9 show the developing of four parameters in LGMD$^+$ during the evolution. In general, the adaptable parameters converge satisfactorily for both the two investigated populations. Though the local thresh-old (T_f) in the FFI-M mechanism shows relatively greater
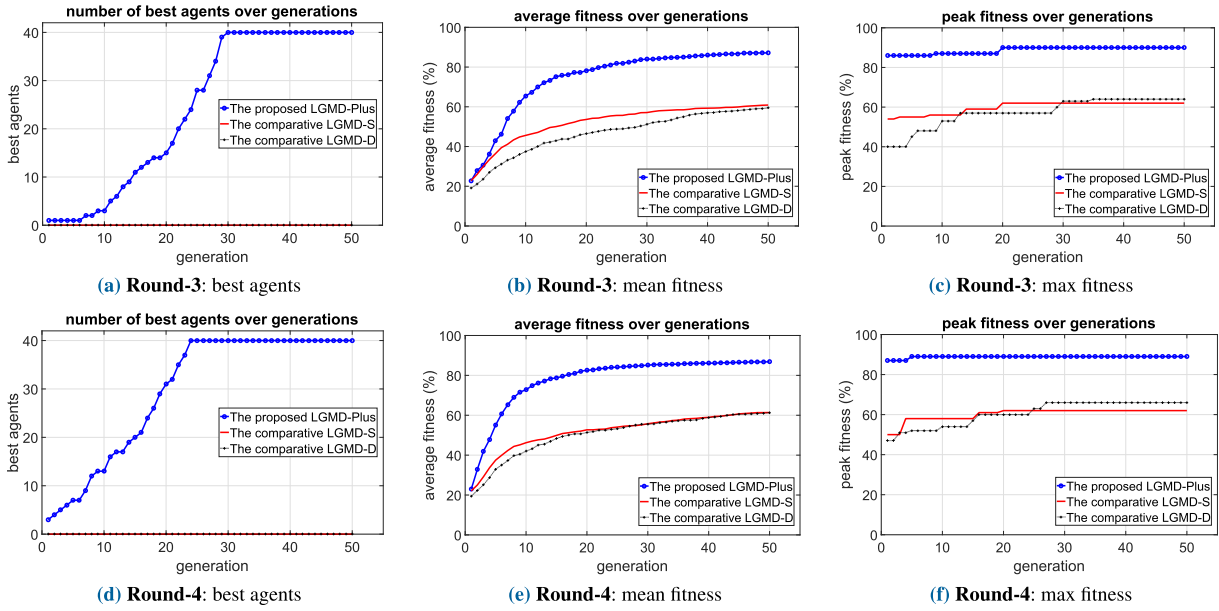
Q. Fu *et al.*: Improved Collision Perception Neuronal System Model With Adaptive Inhibition Mechanism and Evolutionary Learning

IEEE *Access*

FIGURE 8. Individual evolution results (another two rounds) of the three investigated model populations, each with 40 agents over 50 generations.
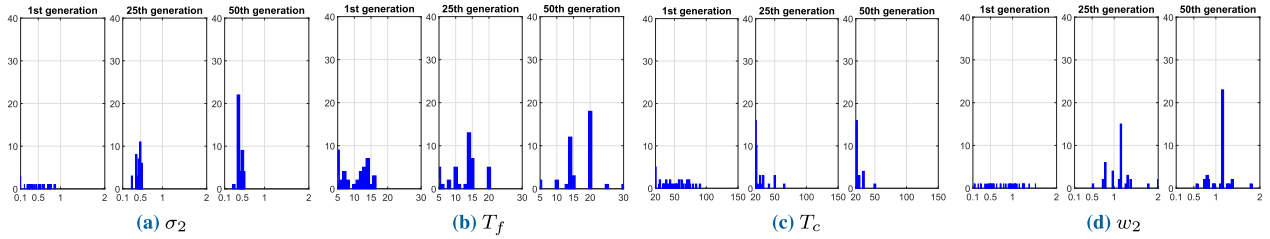

FIGURE 9. Distributions of the four core genes in the investigated LGMD$^+$ population at the 1st, 50th and 100th generations in Fig. 8.

diversity, the majority of adaptable parameters lie within a narrow range, which indicates the developments of LGMD$^+$'s genes remain stable over generations. To sum up, the results of individual evolutions demonstrate the proposed LGMD$^+$ model is more robust and adaptable in various highly variable environments for timely and accurate perception of collision risks, in spite of variations within the investigated adaptable parameters.

2) COMPETITIVE COEVOLUTION RESULTS

Secondly, four rounds of the competitive coevolution results are shown in Fig. 10 and 11, respectively, at two investigated populations. At the beginning of each round, the three groups of models are initialised with a same population. Obviously, the LGMD$^+$ has quickly established the dominant role of collision perception in the evolution environment, with constantly increasing number of participants in the whole population; on the other hand, the two competitive LGMD populations are driven to extinction, after $10 \sim 30$ generations. Consequently, the LGMD$^+$ dominates the whole population. Interestingly, the LGMD-S could occasionally lead the population within the beginning

10 generations (see Fig. 11d). The LGMD$^+$ then takes over the leading role very soon. Notably, even in the 1st generation of the coevolution, the maximum fitness of the LGMD$^+$ population is much higher than the two competitive populations. Not limited to that, the LGMD$^+$ leads the number of 'best agents' in every round of the coevolution that can eventually occupies the total, after $40 \sim 50$ generations. The results demonstrate that the computational structure of the proposed LGMD$^+$ model is more robust with the adaptive inhibition mechanism to survive in the evolution environment, despite variations of the parameters. The LGMD$^+$ can establish solid roles of timely and accurate perception of collision in highly complex-and-changeable visual environments, leaving no opportunity for the competitive LGMD models to develop the same skill.

From the previous research in [29], the robustness of LGMD-S model has been verified due to its simple computational structure that focuses on merely the expanding edges of image, regardless of additional directional information, in comparison with the locust's DSNs neural network models, and their hybrid model. Moreover, the LGMD-D model has also demonstrated the effectiveness of collision detection in
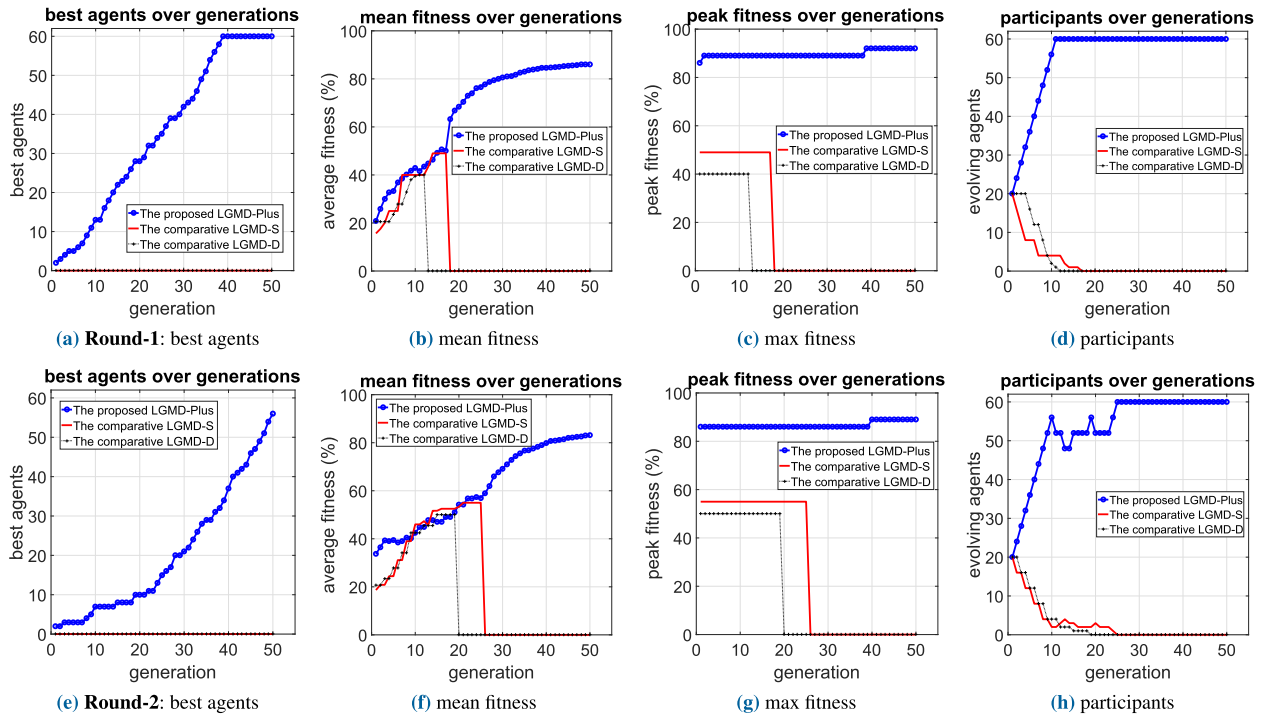
IEEE *Access*

Q. Fu *et al.*: Improved Collision Perception Neuronal System Model With Adaptive Inhibition Mechanism and Evolutionary Learning

FIGURE 10. Coevolution results (two rounds) of the proposed LGMD+ and the comparative LGMD populations, each with 20 agents over 50 generations.
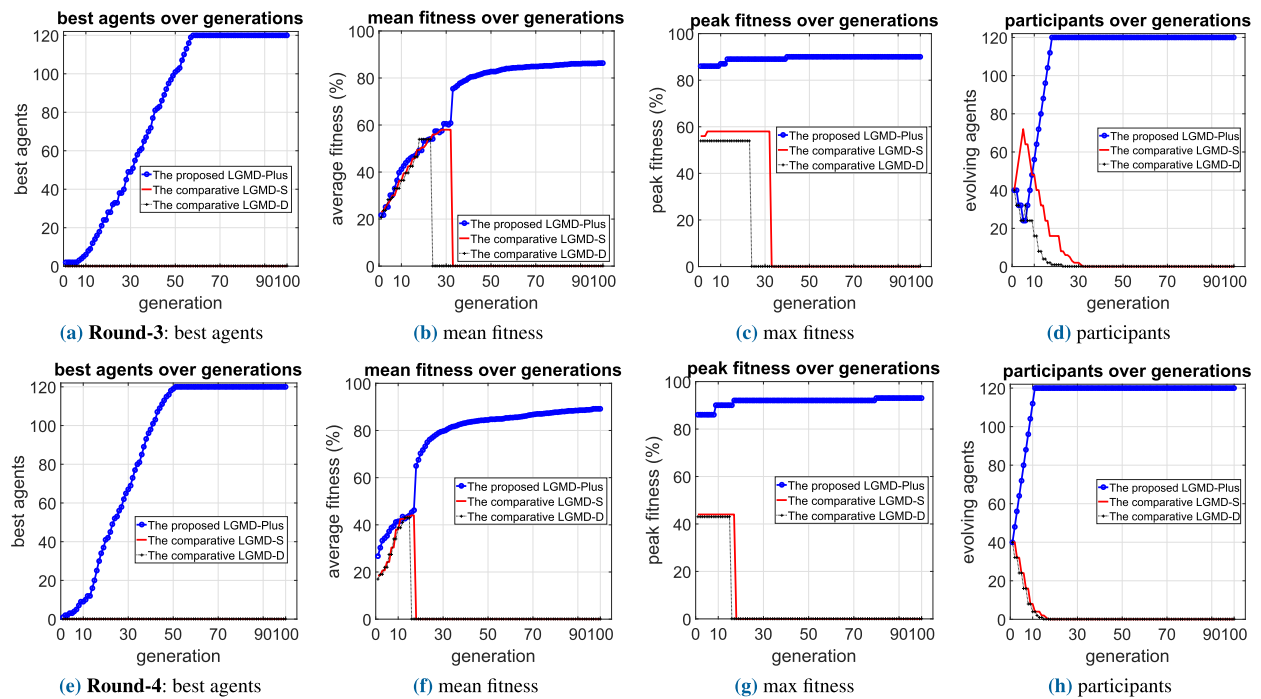

FIGURE 11. Coevolution results (another two rounds) of the three investigated model populations, each with 40 agents over 100 generations.

complex scenes, with preliminary testing on a few driving scenarios [14]. However, we recently have noticed that their abilities, to deal with highly variable statistics of various outdoor environments, are insufficient due to the lack of

adaptive signal processing mechanisms [46]. The coevolution results herein have proved that the proposed modelling of spatiotemporal inhibition dynamics works effectively to improve the LGMD's robustness in more challenging scenes.
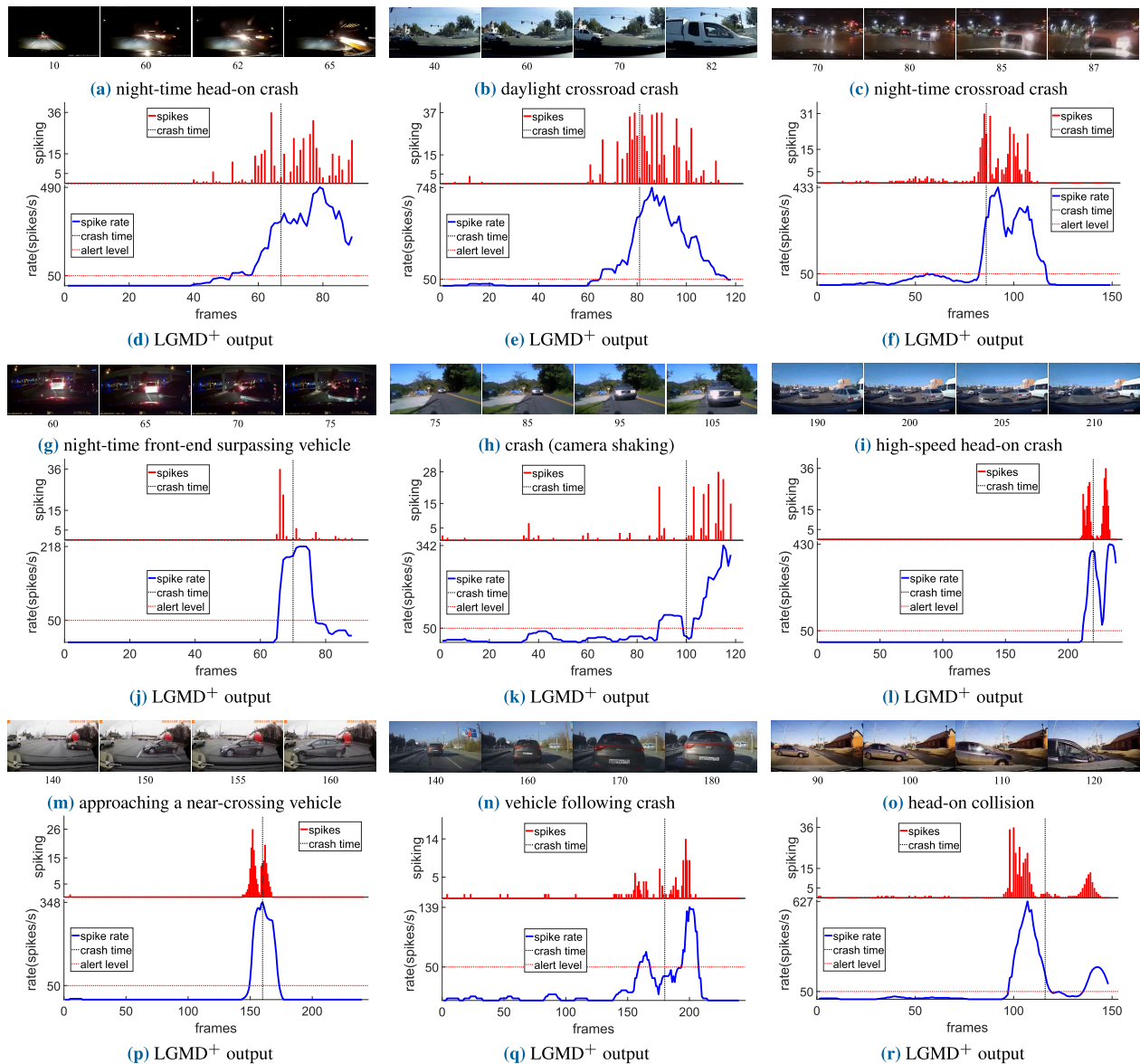
Q. Fu *et al.*: Improved Collision Perception Neuronal System Model With Adaptive Inhibition Mechanism and Evolutionary Learning

IEEE *Access*

FIGURE 12. Outputs of an LGMD$^+$ agent (selected from the last generation) including spikes and firing rate, challenged by various collision cases from the evolution environment. The video clips with frame labels are shown at each top. The horizontal and vertical dashed lines indicate the alert level and the labelled ground truth colliding instant, respectively.

3) PERFORMANCE ON TYPICAL CHALLENGES

To show how the LGMD$^+$ responds to the visual challenges, Fig. 12 and 13 depict a few typical examples including both the collision and non-collision scenarios. Note that the LGMD$^+$ is selected from the evolved generation of best agents. The video clips of evolution environment represent the visual challenges from crowded urban road (Fig. 12b, 12i), night-time driving (Fig. 12a, 12c, 12g) and intense camera vibration (Fig. 12h). The results show that the evolved LGMD$^+$ is effective to extract potential collision risks timely, from different complex backgrounds. The model represents dramatically increasing spike frequency, only before the ground truth colliding moments (Fig. 12). On the other hand, the model almost keeps silent, when

challenged by other non-collision navigations, despite occasionally being elicited individual or sparse spikes (Fig. 13). The results also indicate the LGMD$^+$ has much reduced sensitivity to irrelevant background motion or distractors including peripheral cluttered flows (Fig. 13d), approaching object with deviations from collision (Fig. 13e) and translating stimuli in a proper distance (Fig. 13f).

B. VERIFICATION OF NEW TESTING SCENES

For visual systems with evolutionary learning, the evolution environment is important to determine a structure for certain tasks, i.e., accurate and timely perception of collision in various highly variable environments for this research. The best agents in one specific evolution environment often are not
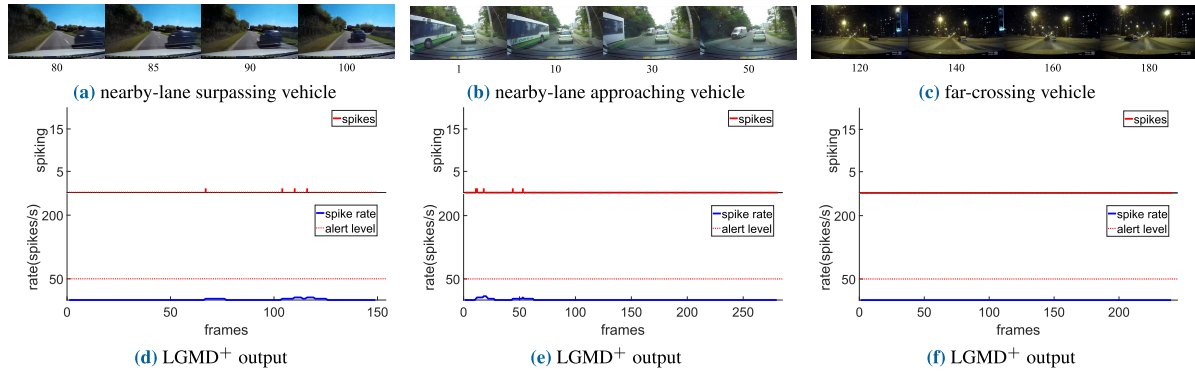
IEEE Access®

Q. Fu *et al.*: Improved Collision Perception Neuronal System Model With Adaptive Inhibition Mechanism and Evolutionary Learning

FIGURE 13. Outputs of an LGMD$^+$ agent (selected from the last generation), challenged by non-collision scenes from the evolution environment.
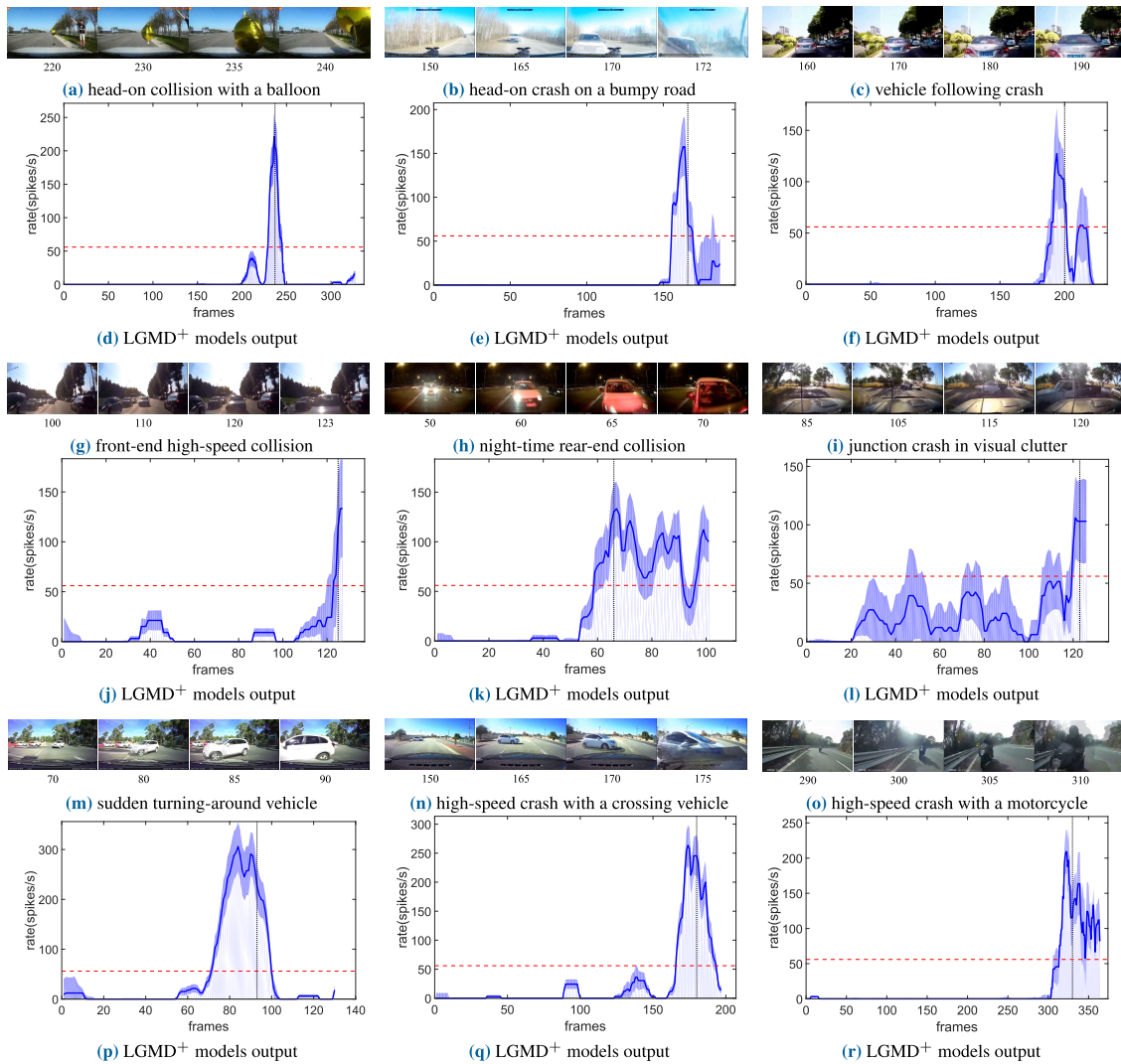

FIGURE 14. Statistical outputs (spike frequency) of the last-generation evolved LGMD$^+$ agents (20 in total), challenged by new testing collision events. The variance of population outputs is shown in shadow.

able to retain satisfactory performance in another unfamiliar environment. To examine whether the proposed LGMD$^+$ model is able to maintain the robust performance via adapting to new complex environments, we have also challenged it with many new on-road driving scenes. The last generation

of the evolved LGMD$^+$ agents together is tested by 87 new scenarios in total, including 51 crash or potential collision scenes and 36 non-collision or near-miss cases. Fig. 14 and 15 illustrate the statistical outputs with variance amongst the 20 tested agents in some typical scenes. The results
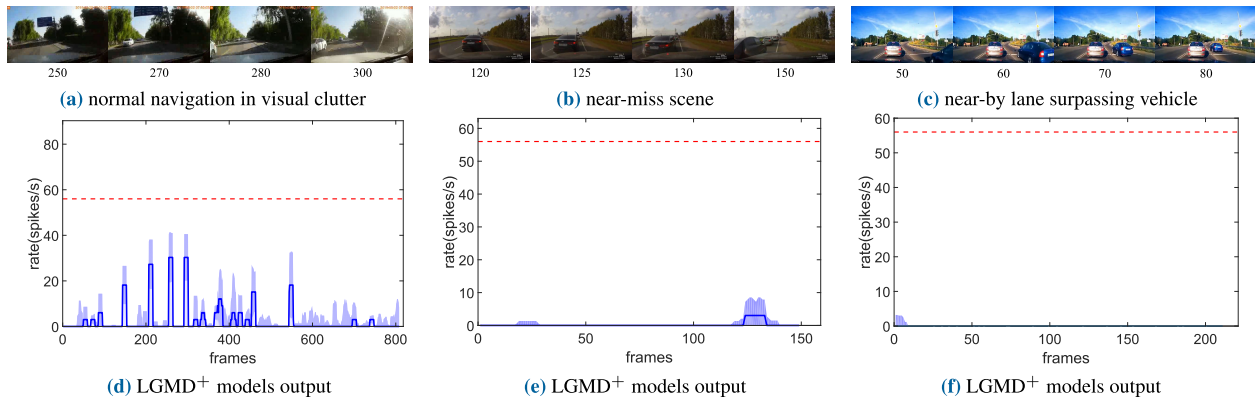
Q. Fu *et al.*: Improved Collision Perception Neuronal System Model With Adaptive Inhibition Mechanism and Evolutionary Learning

IEEE *Access*

(a) normal navigation in visual clutter

(b) near-miss scene

(c) near-by lane surpassing vehicle

(d) LGMD$^+$ models output

(e) LGMD$^+$ models output

(f) LGMD$^+$ models output

FIGURE 15. Statistical outputs (spike frequency) of the last-generation evolved LGMD$^+$ agents (20 in total), challenged by new testing non-collision cases.

TABLE 3. Success rate of the multi-robot arena test.

Agent ID	1	2	3	4	5	6
Total Events	1249	908	1102	1292	1072	1047
Success Avoidance	1148	799	1006	1216	976	935
SR	91.91%	88.0%	91.29%	**94.12%**	91.04%	89.30%

demonstrate that the evolved LGMD$^+$ still secures robust performance against the new visual challenges. More specifically, the vast majority of tested agents can detect collision risks in different dynamic visual backgrounds, timely and accurately, with little variance of model outputs, despite variations of the adaptable parameters between individuals. As illustrated in Fig. 14i and 15a, although some LGMD$^+$ agents could also be activated by visually cluttered flows of high complexity (e.g., the vegetation, shadows, and light flashes), the overall performance is satisfactory. With the proposed spatiotemporal inhibition dynamics, the irrelevant optic flows are largely suppressed, especially in the peripheral areas of vision; whilst the head-on or direct approaching stimuli are sharpened up, with bursting of spikes before collision.
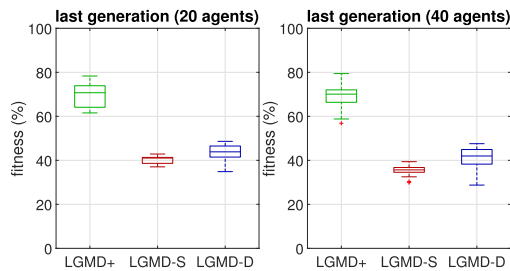

FIGURE 16. Comparative statistical results of the **Fitness** on all (87) new testing scenes: the three evolved LGMD populations are investigated.

Furthermore, Fig. 16 compares the fitness of three evolved LGMD populations, on all the new testing scenes. Intuitively, the proposed LGMD$^+$ models population demonstrates significantly improved robustness (much higher fitness) over the two comparative models, with validation against various new visual challenges.

C. VERIFICATION OF ON-LINE TESTS

After the evolutionary tuning, we further verify the computational simplicity, robustness and flexibility of the LGMD$^+$ with on-board implementation in the micro-mobile robots. The real-time robot experiment lasted for one hour. Fig. 17 articulates the results of multi-robot arena test including collision and avoidance events and density maps. Table 3 elaborates on the SR of every ID-specific robot agent, with which the SR is calculated by taking proportion of success avoidance in total events.

In general, the multi-robot performance is satisfactory to demonstrate the robustness of LGMD$^+$ embodied in robot vision: the overall SR maintains an acceptable level. It can be clearly seen from the density maps in Fig. 17c and 17d that the agents show very high SR near the obstacles and corners, representing greater avoidance densities; however, the collision rate is relatively higher near the edges of arena. The proposed adaptive inhibition mechanism improves the LGMD's selectivity to direct collision dangers, and suppresses other categories of movements including translational optic flows caused by approaching the patterned walls from the side. In addition, the diversity of SR exists between individuals resulting from variations of the adaptable parameters in the last-generation population.

VI. DISCUSSION

Within this section, we discuss 1) characterisation of the LGMD$^+$ and 2) existing challenges.

A. CHARACTERISATION

Through above artificial evolutions in various vehicle driving scenarios, the LGMD$^+$ has demonstrated its improved

IEEE *Access*

Q. Fu *et al.*: Improved Collision Perception Neuronal System Model With Adaptive Inhibition Mechanism and Evolutionary Learning

(a) capture of the arena test with annotations

(b) map of total events

(c) density map of success avoidance
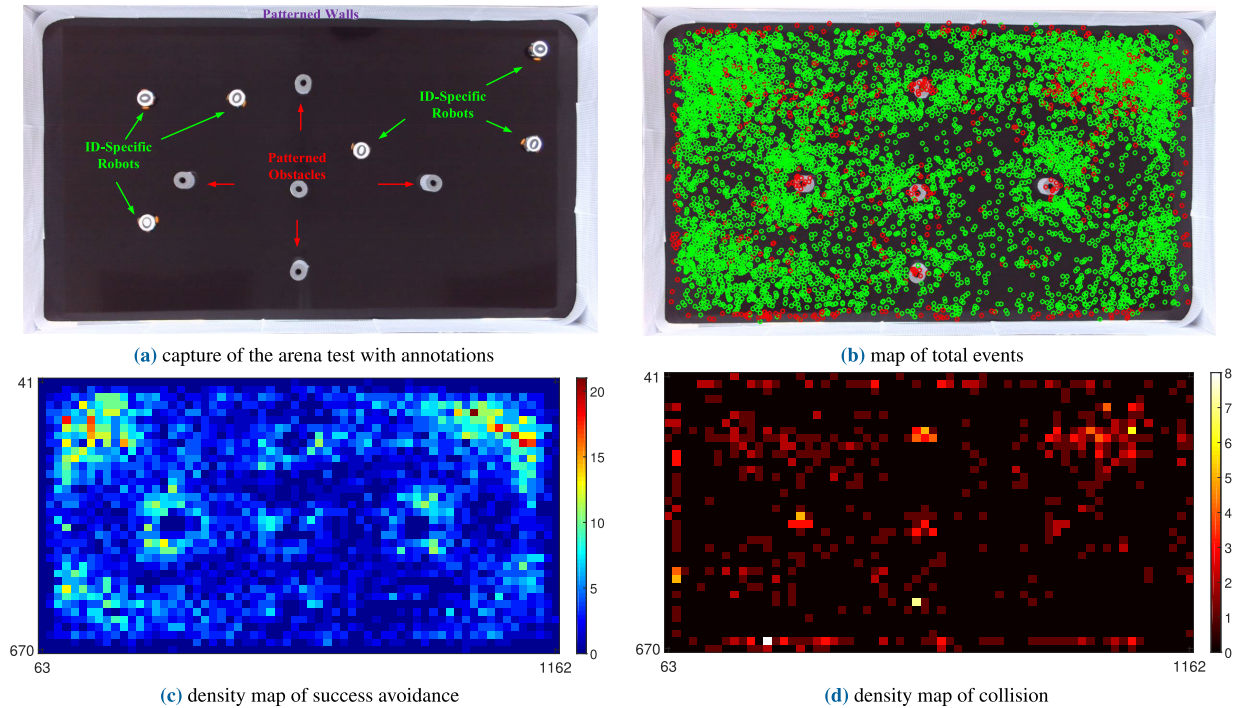

(d) density map of collision

FIGURE 17. Illustrations of the multi-robot arena test results: in (b), green and red circles indicate the avoidance and collision events of all tested agents; in (c)–(d), X and Y axes denote the image coordinates.

robustness compared to the previous related methods. The proposed spatiotemporal inhibition dynamics is novel and crucial, which works effectively to make the visual system more adaptable to highly variable environments. Consequently, the colliding feature by direct approaching objects rather than other categories of movements has been better sharpened up.

After the evolutionary tuning, the LGMD$^+$ with optimised adaptable parameters is effective to deal with many new testing scenes. Moreover, the LGMD$^+$ has also been validated in micro-robot vision for guiding timely and robust collision perception and avoidance. As a promising solution on real world problems, its computational simplicity and flexibility fit with building neuromorphic sensors, either featuring compact size or achieving higher processing speed.

B. CHALLENGES
We have also found some challenges for future work. The LGMD$^+$ model mimics the locust's visual pathways in a feed-forward structure, and avoids segmentation, classification or registration methods for collision perception. As a result, it can not tell what exactly or how many objects are approaching. In our experiments, the LGMD$^+$ is influenced by approaching road or traffic signage like the zebra crossing, and flowing shadows on engine hood (see Fig. 14i). In addition, navigating on curve road could be still challenging the visual system in the background full of quick shifting optic flows; in this case, the adaptive inhibitions could become too strong to suppressing an imminent collision danger.

Similarly, the collision risk could be also concealed during rapid turning. From our perspective, the single neuronal computation is difficult to handle these challenges, whereas the coordination of multiple neural pathways could be effective solutions to encode and separate diverse motion patterns.

Moreover, the varying weather circumstance in outdoor environments is another big challenge. The LGMD$^+$ has shown improved robustness in various backgrounds with good visibility. However, the performance of visual system could be restricted by scenes with poor visibility, e.g., the fog, low-light or heavy-rain conditions. Therefore, a future effort could be introducing the LGMD$^+$ into specialised sensor strategies like the thermal camera system, etc., for addressing these issues and broadening its applications.

VII. CONCLUSION
This paper has presented an improved LGMD neuronal system model, called LGMD$^+$, with adaptive inhibition mechanism and evolutionary learning for timely and accurate perception of collision. Compared to previous methods, the emphasis has been laid on the novel modelling of spatiotemporal inhibition dynamics including a space-varying bias obeying a variant of Gaussian distribution on lateral inhibitions, and a time-varying feed-forward inhibition mediation pathway adjusting the intensity of lateral inhibitions and the latency of local excitations. Accordingly, the model is more adaptable to deal with highly variable statistics of outdoor environments, like the various vehicle driving scenarios. The model shows enhanced selectivity to

Q. Fu *et al.*: Improved Collision Perception Neuronal System Model With Adaptive Inhibition Mechanism and Evolutionary Learning

IEEE*Access*

objects threatening direct collision towards the centre view rather than any other kinds of movements. Evolving with two competitive LGMD models in a variety of complex vehicle scenes, the LGMD$^+$ demonstrates improved robustness. After evolutionary tuning, it is effective to deal with many new challenges. Furthermore, the multi-robot experiments verify its computational flexibility.

REFERENCES

[1] J. S. Kennedy, "The migration of the desert locust (Schistocerca gregaria Forsk.). I. The behaviour of swarms. II. A theory of long-range migrations," *Phil. Trans. Roy. Soc. London. B, Biol. Sci.*, vol. 235, pp. 163–290, May 1951.

[2] M. O'Shea and J. L. D. Williams, "The anatomy and output connection of a locust visual interneurone; the lobular giant movement detector (LGMD) neurone," *J. Comparative Physiol.*, vol. 91, no. 3, pp. 257–266, 1974.

[3] F. C. Rind and D. I. Bramwell, "Neural network based on the input organization of an identified neuron signaling impending collision," *J. Neurophysiol.*, vol. 75, no. 3, pp. 967–985, 1996.

[4] P. J. Simmons and F. C. Rind, "Responses to object approach by a wide field visual neurone, the LGMD2 of the locust: Characterization and image cues," *J. Comparative Physiol.-Sensory, Neural, Behav. Physiol.*, vol. 180, no. 3, pp. 203–214, 1997.

[5] F. C. Rind, S. Wernitznig, P. Polt, A. Zankel, D. Gutl, J. Sztarker, and G. Leitinger, "Two identified looming detectors in the locust: Ubiquitous lateral connections among their inputs contribute to selective responses to looming objects," *Sci. Rep.*, vol. 6, Oct. 2016, Art. no. 35525.

[6] J. M. Yakubowski, G. A. Mcmillan, and J. R. Gray, "Background visual motion affects responses of an insect motion-sensitive neuron to objects deviating from a collision course," *Physiol. Rep.*, vol. 4, no. 10, 2016, Art. no. e12801.

[7] J. Sztarker and F. C. Rind, "A look into the cockpit of the developing locust: Looming detectors and predator avoidance," *Develop. Neurobiol.*, vol. 74, no. 11, pp. 1078–1095, 2014.

[8] P. J. Simmons, F. C. Rind, and R. D. Santer, "Escapes with and without preparation: The neuroethology of visual startle in locusts," *J. Insect Physiol.*, vol. 56, no. 8, pp. 876–883, 2010.

[9] Q. Fu, H. Wang, C. Hu, and S. Yue, "Towards computational models and applications of insect visual systems for motion perception: A review," *Artif. Life*, vol. 25, no. 3, pp. 263–311, Aug. 2019.

[10] Q. Fu, C. Hu, P. Liu, and S. Yue, "Towards computational models of insect motion detectors for robot vision," in *Proc. Towards Auton. Robot. Syst. Conf.*, M. Giuliani, T. Assaf, and M. E. Giannaccini, Eds. Cham, Switzerland: Springer, 2018, pp. 465–467.

[11] M. Hartbauer, "Simplified bionic solutions: A simple bio-inspired vehicle collision detection system," *Bioinspiration Biomimetics*, vol. 12, no. 2, Feb. 2017, Art. no. 026007.

[12] S. B. I. Badia and P. F. M. J. Verschure, "A collision avoidance model based on the lobula giant movement detector (LGMD) neuron of the locust," in *Proc. IEEE Int. Joint Conf. Neural Netw. (IJCNN)*, vol. 3, Jul. 2004, pp. 1757–1761.

[13] S. Yue, F. C. Rind, M. S. Keil, J. Cuadri, and R. Stafford, "A bio-inspired visual collision detection mechanism for cars: Optimisation of a model of a locust neuron to a novel environment," *Neurocomputing*, vol. 69, nos. 13–15, pp. 1591–1598, Aug. 2006.

[14] Q. Fu, C. Hu, J. Peng, and S. Yue, "Shaping the collision selectivity in a looming sensitive neuron model with parallel ON and OFF pathways and spike frequency adaptation," *Neural Netw.*, vol. 106, pp. 127–143, Oct. 2018.

[15] M. S. Keil, E. Roca-Moreno, and A. Rodriguez-Vazquez, "A neural model of the locust visual system for detection of object approaches with real-world scenes," in *Proc. 4th IASTED Int. Conf. Vis., Imag., image Process.*, 2004, pp. 340–345.

[16] R. Stafford, R. D. Santer, and F. C. Rind, "A bio-inspired visual collision detection mechanism for cars: Combining insect inspired neurons to create a robust system," *Biosystems*, vol. 87, nos. 2–3, pp. 164–171, Feb. 2007.

[17] S. Yue and F. C. Rind, "Visual motion pattern extraction and fusion for collision detection in complex dynamic scenes," *Comput. Vis. Image Understand.*, vol. 104, no. 1, pp. 48–60, Oct. 2006.

[18] M. Blanchard, F. C. Rind, and P. F. M. J. Verschure, "Collision avoidance using a model of the locust LGMD neuron," *Robot. Auton. Syst.*, vol. 30, nos. 1–2, pp. 17–38, Jan. 2000.

[19] M. Blanchard, F. C. Rind, and P. F. M. J. Verschure, "How accurate need sensory coding be for behaviour? Experiments using a mobile robot," *Neurocomputing*, vols. 38–40, pp. 1113–1119, Jun. 2001.

[20] S. Yue and F. C. Rind, "Collision detection in complex dynamic scenes using an LGMD-based visual neural network with feature enhancement," *IEEE Trans. Neural Netw.*, vol. 17, no. 3, pp. 705–716, May 2006.

[21] S. B. I. Badia, U. Bernardet, and P. F. M. J. Verschure, "Non-linear neuronal responses as an emergent property of afferent networks: A case study of the locust lobula giant movement detector," *PLoS Comput. Biol.*, vol. 6, no. 3, Mar. 2010, Art. no. e1000701.

[22] C. Hu, Q. Fu, T. Liu, and S. Yue, "A hybrid visual-model based robot control strategy for micro ground robots," in *From Animals to Animats 15*, P. Manoonpong, J. C. Larsen, X. Xiong, J. Hallam, and J. Triesch, Eds. Cham, Switzerland: Springer, 2018, pp. 162–174.

[23] Q. Fu, C. Hu, J. Peng, F. C. Rind, and S. Yue, "A robust collision perception visual neural network with specific selectivity to darker objects," *IEEE Trans. Cybern.*, early access, Dec. 4, 2019, doi: 10.1109/TCYB.2019.2946090.

[24] Q. Fu, S. Yue, and C. Hu, "Bio-inspired collision detector with enhanced selectivity for ground robotic vision system," in *Proc. Brit. Mach. Vis. Conf.* Swansea, U.K.: BMVA Press, 2016, pp. 1–13.

[25] P. Cizek, P. Milicka, and J. Faigl, "Neural based obstacle avoidance with CPG controlled hexapod walking robot," in *Proc. Int. Joint Conf. Neural Netw. (IJCNN)*, May 2017, pp. 650–656.

[26] J. Zhao, X. Ma, Q. Fu, C. Hu, and S. Yue, "An LGMD based competitive collision avoidance strategy for UAV," in *Artificial Intelligence Applications and Innovations*. Cham, Switzerland: Springer, 2019, pp. 80–91.

[27] L. Salt, D. Howard, G. Indiveri, and Y. Sandamirskaya, "Parameter optimization and learning in a spiking neural network for UAV obstacle avoidance targeting neuromorphic processors," *IEEE Trans. Neural Netw. Learn. Syst.*, early access, Oct. 14, 2019, doi: 10.1109/TNNLS.2019.2941506.

[28] H. G. Krapp and F. Gabbiani, "Spatial distribution of inputs and local receptive field properties of a wide-field, looming sensitive neuron," *J. Neurophysiol.*, vol. 93, no. 4, pp. 2240–2253, Apr. 2005.

[29] S. Yue and F. C. Rind, "Redundant neural vision systems—Competing for collision recognition roles," *IEEE Trans. Auton. Mental Develop.*, vol. 5, no. 2, pp. 173–186, Jun. 2013.

[30] W. Green and P. Oh, "Optic-flow-based collision avoidance," *IEEE Robot. Autom. Mag.*, vol. 15, no. 1, pp. 96–103, Mar. 2008.

[31] O. J. N. Bertrand, J. P. Lindemann, and M. Egelhaaf, "A bio-inspired collision avoidance model based on spatial information derived from motion detectors leads to common routes," *PLOS Comput. Biol.*, vol. 11, no. 11, pp. 1–28, 2015.

[32] R. S. A. Brinkworth and D. C. O'Carroll, "Robust models for optic flow coding in natural scenes inspired by insect biology," *PLoS Comput. Biol.*, vol. 5, no. 11, Nov. 2009, Art. no. e1000555.

[33] N. Franceschini, F. Ruffier, and J. Serres, "Insect inspired autopilots," *J. Aero Aqua Bio-Mech.*, vol. 1, no. 1, pp. 2–10, 2010.

[34] N. Franceschini, "Small brains, smart machines: From fly vision to robot vision and back again," *Proc. IEEE*, vol. 102, no. 5, pp. 751–781, May 2014.

[35] J. R. Serres and F. Ruffier, "Optic flow-based collision-free strategies: From insects to robots," *Arthropod Struct. Develop.*, vol. 46, no. 5, pp. 703–717, Sep. 2017.

[36] F. Gabbiani, H. G. Krapp, N. Hatsopoulos, C.-H. Mo, C. Koch, and G. Laurent, "Multiplication and stimulus invariance in a looming-sensitive neuron," *J. Physiol.-Paris*, vol. 98, nos. 1–3, pp. 19–34, Jan. 2004.

[37] S. Yue and F. C. Rind, "A collision detection system for a mobile robot inspired by the locust visual system," in *Proc. IEEE Int. Conf. Robot. Autom. (ICRA)*, Apr. 2005, pp. 3832–3837.

[38] S. Yue, R. D. Santer, Y. Yamawaki, and F. C. Rind, "Reactive direction control for a mobile robot: A locust-like control of escape direction emerges when a bilateral pair of model locust visual neurons are integrated," *Auton. Robots*, vol. 28, no. 2, pp. 151–167, Feb. 2010.

[39] C. Hu, Q. Fu, and S. Yue, "Colias IV: The affordable micro robot platform with bio-inspired vision," in *Proc. Towards Auton. Robot. Syst. Conf.*, M. Giuliani, T. Assaf, and M. E. Giannaccini, Eds. Cham, Switzerland: Springer, 2018, pp. 197–208.

[40] H. Isakhani, N. Aouf, O. Kechagias-Stamatis, and J. F. Whidborne, "A furcated visual collision avoidance system for an autonomous microrobot," *IEEE Trans. Cogn. Devel. Syst.*, vol. 12, no. 1, pp. 1–11, Mar. 2020.

[41] P. Cížek and J. Faigl, "Self-supervised learning of the biologically-inspired obstacle avoidance of hexapod walking robot," *Bioinspiration Biomimetics*, vol. 14, no. 4, May 2019, Art. no. 046002.

[42] Q. Fu and S. Yue, "Modelling LGMD2 visual neuron system," in *Proc. IEEE 25th Int. Workshop Mach. Learn. Signal Process.*, Sep. 2015, pp. 1–6.

[43] Q. Fu, C. Hu, T. Liu, and S. Yue, "Collision selective LGMDs neuron models research benefits from a vision-based autonomous micro robot," in *Proc. IEEE/RSJ Int. Conf. Intell. Robots Syst. (IROS)*, Sep. 2017, pp. 3996–4002.

[44] F. Rind, "Identification of directionally selective motion-detecting neurones in the locust lobula and their synaptic connections with an identified descending neurone," *J. Exp. Biol.*, vol. 149, no. 1, pp. 21–43, 1990.

[45] S. Yue and F. C. Rind, "Postsynaptic organisations of directional selective visual neural networks for collision detection," *Neurocomputing*, vol. 103, pp. 50–62, Mar. 2013.

[46] Q. Fu, N. Bellotto, H. Wang, F. C. Rind, H. Wang, and S. Yue, "A visual neural network for robust collision perception in vehicle driving scenarios," in *Artificial Intelligence Applications and Innovations*. Cham, Switzerland: Springer, 2019, pp. 67–79.

[47] D. E. Goldberg, *Genetic Algorithms in Search, Optimization and Machine Learning*, 1st ed. Boston, MA, USA: Addison-Wesley, 1989.

[48] M. A. Potter and K. A. D. Jong, "Cooperative coevolution: An architecture for evolving coadapted subcomponents," *Evol. Comput.*, vol. 8, no. 1, pp. 1–29, Mar. 2000.

[49] C. D. Rosin and R. K. Belew, "Methods for competitive co-evolution: Finding opponents worth beating," in *Proc. 6th Int. Conf. Genetic Algorithms*, 1995, pp. 373–380.

[50] *Genetic Algorithms Tutorial*. Accessed: Oct. 1, 2019. [Online]. Available: https://www.tutorialspoint.com/genetic_algorithms/index.htm

[51] T. Krajník, M. Nitsche, J. Faigl, P. Vaněk, M. Saska, L. Přeučil, T. Duckett, and M. Mejail, "A practical multirobot localization system," *J. Intell. Robot. Syst.*, vol. 76, nos. 3–4, pp. 539–562, 2014.

HUATIAN WANG (Student Member, IEEE) received the B.Sc. and M.Sc. degrees in applied mathematics from Xi'an Jiaotong University, in 2014 and 2017, respectively. He was awarded the Marie Curie Fellowship to be involved in the EU FP7 Project LIVCODE (295151), as a Research Assistant, in 2016. He is also involved in the EU Horizon 2020 projects STEP2DYNA (691154) and ULTRACEPT (778062), as a Research Assistant, in 2017 and 2019. His research areas include image processing, insect vision, and motion detection.

JIGEN PENG received the B.Sc. degree from Jiangxi University, Nanchang, China, in 1989, and the M.Sc. and Ph.D. degrees from Xi'an Jiaotong University, Xi'an, China, in 1992 and 1998, respectively. He worked with Xi'an Jiaotong University and the City University of Hong Kong, in 2018. He is currently a Professor with the School of Mathematics and Information Science, Guangzhou University, Guangzhou, China. His current research interests include nonlinear functional analysis and applications, machine learning theory, and sparse information processing.

QINBING FU (Member, IEEE) received the B.Sc. degree from the University of Electronic Science and Technology of China, in 2009, the M.Sc. by research degree from the University of Lincoln, in 2014, and the Ph.D. degree from the University of Lincoln, in 2018.

He was awarded the Marie Curie Fellowship to be involved in the EU FP7 Projects EYE2E (269118) and LIVCODE (295151), EU Horizon 2020 projects STEP2DYNA (691154) and ULTRACEPT (778062), as a Research Assistant with the School of Mathematics and Statistics, Xi'an Jiaotong University, Xi'an, China, and the Institute of Microelectronics, Tsinghua University, Beijing, China, from 2014 to 2018. He is currently an Honorary Postdoctoral Research Fellow with the University of Lincoln, a Postdoctoral Research Fellow with the Guangzhou University. His current research interests include neural system modeling, bio-inspired motion vision, bio-robotics, and machine learning. He is a member of the International Neural Network Society (INNS) and the International Society for Artificial Life (ISAL).

SHIGANG YUE (Senior Member, IEEE) received the M.Sc. and Ph.D. degrees from the Beijing University of Technology (BJUT), Beijing, China, in 1993 and 1996, respectively.

He was with BJUT as a Lecturer, from 1996 to 1998, and an Associate Professor, from 1998 to 1999. He was an Alexander von Humboldt Research Fellow with the University of Kaiserslautern, Kaiserslautern, Germany, from 2000 to 2001. He held research positions at the University of Cambridge, Cambridge, U.K., Newcastle University, Newcastle upon Tyne, U.K., and University College London (UCL), London, U.K, from 2002 to 2007. In 2007, he joined the University of Lincoln, Lincoln, U.K., as a Senior Lecturer, and was promoted to a Professor, in 2012, where he is currently a Professor (part-time) with the School of Computer Science. He also holds a Professorship with the Machine Life and Intelligence Research Centre, Guangzhou University, Guangzhou, China, in collaboration with Prof. J. Peng. His current research interests include artificial intelligence, computer vision, robotics, intelligent transportation, brains, and neuroscience. He is a member of the International Neural Network Society (INNS) and the International Society of Bionic Engineering (ISBE).

• • •